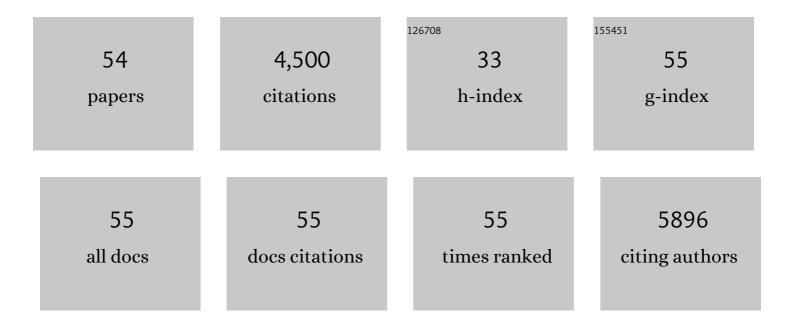
Jiang Deng

List of Publications by Year in descending order

Source: https://exaly.com/author-pdf/10947415/publications.pdf Version: 2024-02-01



LIANC DENC

#	Article	IF	CITATIONS
1	Cooperatively enhanced coking resistance via boron nitride coating over Ni-based catalysts for dry reforming of methane. Applied Catalysis B: Environmental, 2022, 302, 120859.	10.8	61
2	Efficient NO _{<i>x</i>} Abatement over Alkali-Resistant Catalysts via Constructing Durable Dimeric VO _{<i>x</i>} Species. Environmental Science & Technology, 2022, 56, 2647-2655.	4.6	35
3	Synergistic Catalytic Elimination of NO <i>_x</i> and Chlorinated Organics: Cooperation of Acid Sites. Environmental Science & Technology, 2022, 56, 3719-3728.	4.6	41
4	Unraveling the Promotion Effects of Dynamically Constructed CuO _{<i>x</i>} -OH Interfacial Sites in the Selective Catalytic Oxidation of Ammonia. ACS Catalysis, 2022, 12, 3955-3964.	5.5	28
5	Promoting Dry Reforming of Methane Catalysed by Atomicallyâ€Ðispersed Ni over Ceriaâ€Upgraded Boron Nitride. Chemistry - an Asian Journal, 2022, 17, .	1.7	6
6	SO ₂ -Induced Alkali Resistance of FeVO ₄ /TiO ₂ Catalysts for NO <i>_x</i> Reduction. Environmental Science & Technology, 2022, 56, 605-613.	4.6	47
7	SO ₂ -Tolerant Catalytic Reduction of NO _{<i>x</i>} via Tailoring Electron Transfer between Surface Iron Sulfate and Subsurface Ceria. Environmental Science & Technology, 2022, 56, 5840-5848.	4.6	48
8	Unraveling the promotional effects of NiCo catalysts over defective boron nitride nanosheets in dry reforming of methane. Catalysis Today, 2022, 402, 283-291.	2.2	11
9	Coking- and Sintering-Resistant Ni Nanocatalysts Confined by Active BN Edges for Methane Dry Reforming. ACS Applied Materials & Interfaces, 2022, 14, 25439-25447.	4.0	14
10	Sintering- and coking-resistant nickel catalysts embedded in boron nitride supported nickel aluminate spinels for dry reforming of methane. Applied Catalysis A: General, 2022, 642, 118706.	2.2	17
11	Low-Temperature Combustion of Toluene over Cu-Doped SmMn ₂ O ₅ Mullite Catalysts via Creating Highly Active Cu ²⁺ –O–Mn ⁴⁺ Sites. Environmental Science & Technology, 2022, 56, 10433-10441.	4.6	40
12	Coking-resistant dry reforming of methane over Ni/γ-Al2O3 catalysts by rationally steering metal-support interaction. IScience, 2021, 24, 102747.	1.9	34
13	Efficient catalytic combustion of toluene at low temperature by tailoring surficial PtO and interfacial Pt-Al(OH)x species. IScience, 2021, 24, 102689.	1.9	24
14	High-Performance Binary Mo–Ni Catalysts for Efficient Carbon Removal during Carbon Dioxide Reforming of Methane. ACS Catalysis, 2021, 11, 12087-12095.	5.5	61
15	SO ₂ -Tolerant NO _{<i>x</i>} Reduction by Marvelously Suppressing SO ₂ Adsorption over Fe _{1´} Ce _{1â^´l´} VO ₄ Catalysts. Environmental Science & Technology, 2020, 54, 14066-14075.	4.6	76
16	Selective catalytic oxidation of NH ₃ over noble metal-based catalysts: state of the art and future prospects. Catalysis Science and Technology, 2020, 10, 5792-5810.	2.1	82
17	Boosting Toluene Combustion by Engineering Co–O Strength in Cobalt Oxide Catalysts. Environmental Science & Technology, 2020, 54, 10342-10350.	4.6	165
18	Unraveling the effects of the coordination number of Mn over α-MnO2 catalysts for toluene oxidation. Chemical Engineering Journal, 2020, 396, 125192.	6.6	110

JIANG DENG

#	Article	IF	CITATIONS
19	Coking-resistant dry reforming of methane over BN–nanoceria interface-confined Ni catalysts. Catalysis Science and Technology, 2020, 10, 4237-4244.	2.1	37
20	Boosting the Alkali/Heavy Metal Poisoning Resistance for NO Removal by Using Iron-Titanium Pillared Montmorillonite Catalysts. Journal of Hazardous Materials, 2020, 399, 122947.	6.5	34
21	Promotional effects of B-terminated defective edges of Ni/boron nitride catalysts for coking- and sintering-resistant dry reforming of methane. Applied Catalysis B: Environmental, 2020, 267, 118692.	10.8	96
22	Turning on electrocatalytic oxygen reduction by creating robust Fe–N _x species in hollow carbon frameworks <i>via in situ</i> growth of Fe doped ZIFs on g-C ₃ N ₄ . Nanoscale, 2020, 12, 5601-5611.	2.8	29
23	Promoting toluene oxidation by engineering octahedral units <i>via</i> oriented insertion of Cu ions in the tetrahedral sites of MnCo spinel oxide catalysts. Chemical Communications, 2020, 56, 6539-6542.	2.2	25
24	Creating Sandwich-like Ti ₃ C ₂ /TiO ₂ /rGO as Anode Materials with High Energy and Power Density for Li-Ion Hybrid Capacitors. ACS Sustainable Chemistry and Engineering, 2019, 7, 15394-15403.	3.2	57
25	Annular Mesoporous Carbonaceous Nanospheres from Biomass-Derived Building Units with Enhanced Biological Interactions. Chemistry of Materials, 2019, 31, 7186-7191.	3.2	28
26	Fe-, N-Embedded Hierarchically Porous Carbon Architectures Derived from FeTe-Trapped Zeolitic Imidazolate Frameworks as Efficient Oxygen Reduction Electrocatalysts. ACS Sustainable Chemistry and Engineering, 2019, 7, 19268-19276.	3.2	21
27	Oxygen Groups Immobilized on Micropores for Enhancing the Pseudocapacitance. ACS Sustainable Chemistry and Engineering, 2019, 7, 11407-11414.	3.2	23
28	Methane dry reforming over boron nitride interface-confined and LDHs-derived Ni catalysts. Applied Catalysis B: Environmental, 2019, 252, 86-97.	10.8	126
29	Structural Evolution of Metal (Oxy)hydroxide Nanosheets during the Oxygen Evolution Reaction. ACS Applied Materials & Interfaces, 2019, 11, 5590-5594.	4.0	58
30	Low-crystalline tungsten trioxide anode with superior electrochemical performance for flexible solid-state asymmetry supercapacitor. Journal of Materials Chemistry A, 2018, 6, 8986-8991.	5.2	58
31	Improved catalytic activity and stability for hydrogenation of levulinic acid by Ru/N-doped hierarchically porous carbon. Molecular Catalysis, 2018, 448, 100-107.	1.0	49
32	Efficient synthesis of ultrafine Pd nanoparticles on an activated N-doping carbon for the decomposition of formic acid. Catalysis Communications, 2018, 108, 55-58.	1.6	48
33	Oxygen vacancies on the surface of H _x WO _{3â^'y} for enhanced charge storage. Journal of Materials Chemistry A, 2018, 6, 6780-6784.	5.2	36
34	High-performance flexible redox supercapacitors induced by methylene blue with a wide voltage window. Sustainable Energy and Fuels, 2018, 2, 357-360.	2.5	27
35	Sustainable and scalable synthesis of monodisperse carbon nanospheres and their derived superstructures. Green Chemistry, 2018, 20, 4596-4601.	4.6	31
36	Shape Engineering of Biomassâ€Derived Nanoparticles from Hollow Spheres to Bowls through Solventâ€Induced Buckling. ChemSusChem, 2018, 11, 2540-2546.	3.6	37

JIANG DENG

#	Article	IF	CITATIONS
37	Asymmetric Flasklike Hollow Carbonaceous Nanoparticles Fabricated by the Synergistic Interaction between Soft Template and Biomass. Journal of the American Chemical Society, 2017, 139, 2657-2663.	6.6	139
38	Ultramicroporous carbon cloth for flexible energy storage with high areal capacitance. Energy Storage Materials, 2017, 7, 216-221.	9.5	94
39	Organic-acid-assisted synthesis of a 3D lasagna-like Fe-N-doped CNTs-G framework: An efficient and stable electrocatalyst for oxygen reduction reactions. Nano Research, 2017, 10, 1258-1267.	5.8	28
40	Cooperative chiral salen Ti ^{IV} catalyst supported on ionic liquid-functionalized graphene oxide accelerates asymmetric sulfoxidation in water. Catalysis Science and Technology, 2017, 7, 5944-5952.	2.1	16
41	Morphology Dynamics of Single-Layered Ni(OH) ₂ /NiOOH Nanosheets and Subsequent Fe Incorporation Studied by <i>in Situ</i> Electrochemical Atomic Force Microscopy. Nano Letters, 2017, 17, 6922-6926.	4.5	121
42	Efficient Catalytic Hydrodeoxygenation of Aromatic Carbonyls over a Nitrogenâ€Đoped Hierarchical Porous Carbon Supported Nickel Catalyst. ChemistrySelect, 2017, 2, 8486-8492.	0.7	29
43	Reactive Fe-Sites in Ni/Fe (Oxy)hydroxide Are Responsible for Exceptional Oxygen Electrocatalysis Activity. Journal of the American Chemical Society, 2017, 139, 11361-11364.	6.6	532
44	Ultraviolet-responsive self-assembled metallomicelles for photocontrollable catalysis of asymmetric sulfoxidation in water. RSC Advances, 2017, 7, 54570-54580.	1.7	7
45	In Situ Synthesis of Chitin-Derived Rh/N–C Cataylsts: Efficient Hydrogenation of Benzoic Acid and Derivatives. ACS Sustainable Chemistry and Engineering, 2017, 5, 9894-9902.	3.2	44
46	Hydrothermal synthesis of manganese oxide encapsulated multiporous carbon nanofibers for supercapacitors. Nano Research, 2016, 9, 2672-2680.	5.8	41
47	Effects of Cellulose, Hemicellulose, and Lignin on the Structure and Morphology of Porous Carbons. ACS Sustainable Chemistry and Engineering, 2016, 4, 3750-3756.	3.2	261
48	Nitrogen-doped flower-like porous carbon materials directed by in situ hydrolysed MgO: Promising support for Ru nanoparticles in catalytic hydrogenations. Nano Research, 2016, 9, 3129-3140.	5.8	24
49	3D-interconnected hierarchical porous N-doped carbon supported ruthenium nanoparticles as an efficient catalyst for toluene and quinoline hydrogenation. Green Chemistry, 2016, 18, 6082-6090.	4.6	121
50	Acid Induced Self-Assembly Strategy to Synthesize Ordered Mesoporous Carbons from Biomass. ACS Sustainable Chemistry and Engineering, 2016, 4, 4473-4479.	3.2	48
51	Biomass-derived carbon: synthesis and applications in energy storage and conversion. Green Chemistry, 2016, 18, 4824-4854.	4.6	735
52	Inspired by bread leavening: one-pot synthesis of hierarchically porous carbon for supercapacitors. Green Chemistry, 2015, 17, 4053-4060.	4.6	397
53	Controlled synthesis of sustainable N-doped hollow core-mesoporous shell carbonaceous nanospheres from biomass. Nano Research, 2014, 7, 1809-1819.	5.8	52
54	Controlled Synthesis of Ordered Mesoporous Carbohydrate-Derived Carbons with Flower-like Structure and N-Doping by Self-Transformation. Chemistry of Materials, 2014, 26, 6872-6877.	3.2	88